Observation of Shoemaker-Levy Impacts by the Galileo Photopolarimeter Radiometer

Terry Z. Martin[1]
Glenn S. Orton[1]
Larry D. Travis[2]
Leslie K. Tamppari[1]
Ian Claypool[1]

[1]*Jet Propulsion Laboratory,*
4800 Oak Grove Dr.
MS 169-237
California Institute of Technology,
Pasadena CA 91109

[2]*Goddard Institute for Space Studies*
2880 Broadway
New York City NY 10025

Submitted to Science Dec. 81994

Manuscript pages: 17

Figures: 6

Tables: 1

Suggested running head: Galileo Shoemaker-Levy observations

Direct correspondence to:

Terry Z. Martin
Mail stop 169-237
Jet Propulsion Laboratory
4800 Oak Grove Dr.
Pasadena CA 91109
(818) 354-2178
FAX: (818) 393-4619
Terry .Z.Martin@jpl.nasa.gov

Abstract

The Galileo Photopolarimeter Radiometer (PPR) experiment took direct high-speed photometric observations at 678 and 945 nm of several SL9 fragment impacts with Jupiter. Initial flashes occurred at (G) July 18, 07:33:32, (H) July 18, 19:31:58, (L) July 19, 22:16:48; and (Q1) July 20, 20:13:52 (equivalent UTC observed at earth), with relative peak 945-rim brightnesses of 0.87, 0.67, 1.00 and 0.42, respectively. These lightcurves show a 2-see rise to maximum, a 10-sec plateau and an accelerating falloff. The Q1 event, observed at both wavelengths, yields a color temperature of more than 10,000 K at its peak.

INTRODLJCTION

The impacting of Comet Shoemaker-Levy 9 ("S1.9") into Jupiter in July 1994 was an extraordinary event, stimulating an unparalleled set of astronomical observations, The instrument complement of the Galileo spacecraft, on its way to a December 1995 orbit insertion at Jupiter, was able to observe the impact events from a unique vantage point above the dawn terminator (Fig. 1). The Photopolarimeter Radiometer (PPR) (1), a single field-of-view instrument, employs a rotating filter wheel covering a variety of wavelengths in the visible and near infrared for photometric and polarimetric remote sensing of Jupiter's atmosphere and satellites.

For the observations of SL9, the PPR was used as a high-speed photometer, as it was important to maximize the chance of observing the radiation associated with the impact events, given considerable uncertainty about their magnitude, timing, and duration. Brief, bright emission from a very small area was expected for the "meteor flash" as the comet fragments passed through the atmosphere (2). With the comet moving at 60 km/see, its passage through the atmosphere could be short enough that the detectable signal might be lost while rotating between filters. Consequently, single filter measurements with a 0.23 sec sample time were employed for most of the observed impacts.

Among the available wavelengths, two of the three polarimeter filters were selected: 678 and 945 nm (with bandwidths of 9 and 11 nm, respectively), near the peak sensitivity of the silicon diode detectors. Most events were observed at 945 nm alone, offering the possibility of detecting thermal emission from an upwelling fireball, which at some 3000 K (2) would be cooler than the entry meteor flash. For fragment Q1, however, measurements alternated at 678 and 945 nm, with a sample period of 1.26 sec at either wavelength.

Radiation passes through a Wollaston prism in the PPR in order to separate orthogonal polarizations, which are sensed by separate detectors (1). These simultaneous measurements afforded an enhanced ability to confirm the reality of detections, since the signal for a real event would appear in both channels, in contrast to random noise or spikes produced by cosmic rays hitting the silicon diode detector; the impact-induced radiation was not likely to be polarized.

At a distance of 1.6 AU from Galileo, Jupiter subtended only 0.6 mrad within the PPR 2.5 mrad diameter field (Fig. 1). With no scan platform motion required (3), and no use of the tape recorder (4), the PPR observations were sufficiently benign to be approved by the Project at times when Galileo was not in contact with any ground station. Impact events B, H, L, Q1, and S were selected for the memory-buffered approach (4). For the C, G, and R events, the PPR was set up to record data simultaneously with the infrared and ultraviolet spectrometer measurements (5). The R data on tape are not yet available.

Whether an impact event was detected depended on three factors:

1. Movement of the actual impact time relative to fixed observing time. The start and end times for the observation were fixed in mid-June by the spacecraft planning schedule.

2. Brightness of the impact, influencing signal level.

3. Amount of the stored data that could be returned given downlink communication time available.

OBSERVATIONS

Among the set of memory -buffered obsmvations, definite signals were found for H, L, and Q1 (6; Fig. 2-3). These events were all much shorter than the observed time span (Table 1). The 1 σ noise level at 945 nm for all observations was 1.2 data numbers (DN) after averaging the two polarization channel signals together without smoothing. This is about 0.5% of the integrated brightness of Jupiter at 945 nm.

All of the events detected show a rise to maximum signal within 2 seconds, at which time there is a sudden slope change at the peak intensity. All of the 945-rim measurements bear a similar shape, with about a 10-sec plateau prior to falloff. The maximum duration of detected light is 35 sec for L. Data returned from the G impact, although sampled less frequently, show the same general behavior as the others (Fig. 4). There is a suggestion of secondary flashes in the 3 minutes following the main G flash. However, examination of the two PPR channels shows a lack of correlated signals during this period, and it is unlikely that these peaks are real. It should be pointed out that there is no structure in the data indicating a separate detection of a “meteor” and a “fireball” phase, except perhaps for the slope change.

The 678 nm data for Q1 differ in that the signal decays faster (Fig. 5). We note that the time-drift images of impacts K and N at 890 nm by the Solid State Imaging instrument on Galileo (7) show a comparable duration to our 945 nm data, and a similar shape. The SS1 sequence of W images at 559 nm (7) show a rise and fall within about 5 see, which is similar to the Q1 678 nm behavior. There is an unidentified spike in the Q 1 data about 1.5 min after the principal event seen in four channels (Fig. 3); this spike appears

only in the two 678 nm channels, and those amplitudes differ by over a factor of two. Although the amplitudes are well above noise levels, the brevity of the signature and its dissimilar amplitudes suggest this may be a cosmic ray event affecting the two independent detectors. No other event of this kind is seen in the entire SL9 data set.

ANALYSIS

Two possible interpretations of the PPR data were initially conceived:

1. The flashes represent the hot meteor phase of the fragments' demise, with a duration indicative of the time for the glowing trail material to radiate its energy.

2. The PPR signal represents ***only*** the "fireball" phase: the upwelling or expansion of hot material after the meteor deposits its energy.

Clues to the origin of the light seen by the PPR can be found in the absolute intensities, in the ratio of intensities at different wavelengths, and in the correlation with other data sets.

The peak absolute signal levels observed by the PPR at 945 nm represent about 6% of the signal from Jupiter itself for the L event. The signal can be modelled by

$$S_{945} = B_{945}(T(t)).a.)(t), \qquad (1)$$

where B(T(t)) is the time-dependent Planck function and ω(t) is the effective solid angle subtended by the emission. The peak L signal is fit for either of these two distinct cases:

1. A meteor flash having T=10000 K and the solid angle of a 150 km^2 area. This area could be a "pencil" of dimensions 2,5 by 60 km, for example.

2. A fireball having T=3000 K and the solid angle of an area 400 km^2 in size.

From this information alone, it would be difficult to establish a mechanism for the flash.

A substantial clue to the interpretation of the PPR signals is provided by the 678 and 945 nm flux ratio for Q 1. The ratio indicates temperatures near 18000 K, if blackbody emission is assumed (Fig. 5; note 8). At such temperatures, a source area near 5 km^2 is adequate. 'I'he high emission at 678 relative to that at 945 nm implies a hot and compact phenomenon being responsible for the earliest few seconds of the PPR light curve. The rapid dropoff of radiation at 678 nm indicates a rapid cooling phase, as the peak of the blackbody radiation shifts to longer wavelengths. This behavior is consistent with the brevity of the 229-nm detection by the Galileo Ultraviolet Spectrometer experiment for G (9) and the brief 559-rim peak measured by the SS1 for W (7).

The 678 nm to 945 nm flux ratio drops to a value consistent with blackbody temperatures less than 4000K and an area on the order of 600 km^2 within 10 seconds. Initial high temperature and small solid angle are also suggested for the G impact by the ratio of the Galileo UVS 229 nm flux to that detected by the PPR at 945 nm during the rise to maximum signal (9). Behavior of the Near-IR Mapping Spectrometer spectra obtained seconds later for G are also consistent with an expanding, cooling, blackbody source with an initial temperature above 5000 K, going down to 450 K in just over a minute (1 O). The atmospheric pressure levels implied from the NIMS methane band data, when extrapolated backward to the time of the PPR peak, are near 50 mb, well below where a meteor trail would be found.

Could the first few seconds of the PPR flashes be due to the meteor phase? That phase of the impacts should resemble large terrestrial meteor events; ablation by either Jovian H_2 or terrestrial N2 would in either case

produce a hot vaporized layer of impactor material. Terrestrial meteors display a rich spectrum of metallic lines corresponding to excitation temperatures in the several thousand K range (11). Most of these lines arein the blue region, with only weak continuum in the red and infrared (12). Consequently, we expect the meteor phase to be dim at the PPR-detected wavelengths, as well as those used by the SS1 camera (13).

It also seems unlikely that the intensity of the meteor phase would so nicely merge into that of the fireball phase that follows. Note that the light curve shapes are very similar for four events of differing magnitude (Fig. 6). The only indication of a separation is the aforementioned slope change, which could indicate termination of the trail or disappearance below clouds.

Thus, the PPR measurements, together with those of the other Galileo experiments, imply a continuous impact radiation event, with no clear distinction between an impacting meteor flash and subsequent fireball. The three-dimensional modelling of the impacts by Crawford *et al* (2) imply that the meteor entry above the level of obscuring clouds would be followed by immediate expansion of the upper portion of the entry tube into a hot, compact fireball, aided perhaps by subsequent rebound of material from further down the tube. In this comparison, the sharp initial rise of the PPR data may correspond to the fast passage of the fragment through the visible part of the atmosphere. The rise would be caused by a growing solid angle of the entry tube, and the increasing frictional discharge of the fragment's kinetic energy into ablation heat. The abrupt cessation of the intensity rise is ascribed to either the bolide passing below a cloud layer, or to final breakup of the body. The following part of the PPR curve, which arises from a prompt "fireball" phenomenon, is simply the contribution of two competing terms: a cooling Planck emission and a growing solid angle, as in Equation 1. The balance of these terms produces the flat part of the curve at 945 nm, and the acceleration downward of the signal indicates the growing

dominance of the cooling. Note that it is not necessary to conclude from the Crawford et *al* model that PPR detects the meteor phase emission.

Interpreting comparisons with simultaneous earth-based observations is very important but by no means straightforward. Terrestrial observations attest to the complicated nature of the impacts, which may in some cases have involved tidally disrupted portions of the main impacting fragment. Sensitive near-infrared (-2 μm) light curves of several impacts from various observatories typically show two low-amplitude events before the main infrared brightening (14,1 5,16, 17). One interpretation of these three events is that they arise from (a) the impact bolide, (b) the plume and fireball upwelling over the horizon, and (c) the thermalization of the kinetic energy of the particles upon re-entry into the upper atmosphere.

The prospect is extremely intriguing that the initial bolide could be seen from earth, either from light refracted past the limb or, more likely, reflected off an incoming dust train. Verification of the simultaneity with Galileo observations is important for this interpretation. For the L impact, both Calar Alto (14) and Pic-du-Midi (15) measured the first of these small signals near the time of the PPR detection. The first observation of the H impact by Calar Alto (14), on the other hand, appears at 19:33, a minute after the PPR signal, although these may be consistent, given the ±1 min timing accuracy of these Calar Alto observations. For the G impact, the Anglo-Australian Telescope (18) observed a faint point-like source on the limb at 7:32:58, coincident with the PPR time to within the 2-rein AAT sampling interval. These comparisons are all consistent with the impact flashes being observable from the earth. The coincidence of a feature above the limb at the G impact site in an 888 nm filter exposure made by the Hubble Space Telescope Wide-field/Planetary Camera between 7:33:15 and 7:33:45 (19) lends weight to the interpretation that the initial flash observed from the earth was fireball radiation reflected off a trailing dust cloud. Its

integrated brightness is much less than that measured by the PPR at nearly the same wavelength within the same time frame, implying that most of the radiation detected by the PPR originated below the HST-observed limb. Furthermore, its appearance at the limb 400 km above the 100-mbar level, seconds after the PPR observations, implies a time interval too short for a fireball to well up, assuming a speed on the order of the ~10 km/see velocities responsible for the observed ballistic trajectories of the plume material at subsequent times (19). Obviously, the most complete picture of the first few seconds of the impact events will arise from detailed comparisons between the PPR and other Galileo observations and a large suite of terrestrial measurements at these and later times, together with models of the impact phenomenon.

We can readily determine an upper limit for the flux reflected from the closest Galilean satellite, Io, for the initial flash. The peak flux density for fragment L observed at a distance of 1.6 AU by the PPR at 945 nm wavelength is 2.7 x 10^{-15} W cm^{-2} rim-l (Fig. 6). Scaling that value to Io's distance from Jupiter's "surface" (3.52 x 10^5 km), we get 1.26 x 10^{-9} W cm^{-2} rim-l, assuming isotropic emission from the impact point. Dividing this by the solar flux density at Jupiter at 945 nm (3.03 x 10^{-6} W cm^{-2} rim-l; ref. 20), we obtain 4.15 x 10^{-4}. This maximum brightening that might be expected for Io would be difficult to detect, and is consistent with the apparent lack of such reflected impact "flashes".

Although we intended to derive absolute mass estimates from the PPR flash intensities, it is now unclear if that will be possible, since much of the energy deposition may be hidden from view for deeper-penetrating fragments. Whatever its value, we can however state a relative brightness based on the 945 nm data in hand. Using the peak values of the 945 nm

signal, we find L, G, H, and Q1 to have relative brightness of 2.4:2.1:1.6:1.0. The HST observations of the impact sites (19) provide a qualitative hierarchy in which the G, K and L impact sites have the highest associated energy because of their large ejecta, central dark region more than 10,000 km in diameter, and multiple impact waves. The H impact site has a central dark region between 4000 and 8000 km in size, medium ejects and a single impact wave, and Q1 has a central dark region less than 3000 km with no ejects and no observed impact wave. These are consistent with the ordering in energy that can be established with the PPR (and other Galileo) measurements. Further earth-based measurements of comparative phenomena, such as amount of NH3 gas upwelled, column abundance of particulate generated or amplitude of temperature perturbation can provide significant additional constraints on the incoming fragment energy. On the other hand, pre-impact HST observations of the individual cometary fragments give brightnesses (21) for L, G, H and Q1, of 1.00, 1.33,0.80 and 1.40, respectively. These are in obvious disagreement with our ordering, and imply that a significant component of the observed comet brightness was contributed by particles that did not contribute substantially to the kinetic energy of the incoming fragment. The breakup of Q also suggests that the impactors are not structurally identical to the earlier fragments.

REFERENCES AND NOTES

1. E. Russell *et al, Sp. Sci. Rev,* 60, 531 (1992).

2. M. Boslough, D.A. Crawford, T.G. Trucano, and A.C. Robinson, *EOS* 75, 305 (1994). D.A. Crawford, M. Boslough, T.G. Trucano, and A.C. Robinson, *Shock Waves* 4,47 (1994). K. Zahnle and M.-M. Mac Low, *Icarus* 108, 1 (1994). T. Takata, T. J. Ahrens, J.D. O'Keefe, and G.S. Orton, *Icarus* 109, 3 (1994).

3. The pointing stability of the Galileo scan platform has evolved to the point that targetting within the 2.5 rnrad PPR field of view can be reliably accomplished. Moreover, the viewing can be held to within about 1 mrad for long periods. Thus, it was practical to point at Jupiter and stare with the PPR for the duration desired. The observed signal levels and their constancy imply steady pointing at Jupiter was achieved for the desired observing period.

4. The Galileo main antenna failed to open properly in 1992, leaving the spacecraft with diminished communications capacity. It was therefore necessary to plan for extended playback (about six months) of SL9 data acquired on the tape recorder for most of the remote sensing observations. However, an additional mechanist was available for instruments with low data rates such as the PPR (216 bps). With some reprogramming, the PPR data were captured in the flight computer's memory, and then read out using existing memory verification procedures. With about 44 Kbytes of memory available, about 41 minutes of PPR data was stored in one sequence. At a nominal downlink rate of 10 bps, these data were sent to the Earth in about 12 hours. Having this early delivery of data from some of the impacts was intended to facilitate determination of relative timing of the impacts, and thus enhance the ability to read out from the tape recorder selected data from other experiments, in the event that no earthbased data were available to establish impact times.

5. A repetitive scanning motion used for G and R enabled the two slit spectrometers (UVS and NIMS) to cover platform pointing error, The PPR data for G therefore consist of several on-Jupiter samples obtained for each 5.3 *sec* scan period, at 945 nm. Imaging

sequences for events D, E, K, N, and W were done in modes that prevented useful simultaneous PPR measurements. Constraints on available time for telemetry precluded return of data from the C event.

6. We believe that the fragment B impact was coveredtimewise but was too small to be detected. Data recorded for P were considered unlikely to be useful, given reports from ground-based observers and the HST. Fragment S may have been detectable but apparently impacted at a time too early for our fixed observation window.

7. For K, the Galileo camera shutter was held open as Jupiter was slewed across the field, providing a time-resolved trace of the flash brightness. For W, separate images of Jupiter were made each 2,.3 sec. M. J. S. Belton, C. R. Chapman, T. V. Johnson, C. M. He ffeman, K, P. Klaasen, *Bull, Amer. Astron. Soc.,* in press.

8. The color temperature derived from the ratio of the 678 to 945 nm signal for event Q1 is highly sensitive to the absolute radiometric calibration of the PPR at these wavelengths. Although inflight observations of Sirius confirm the preflight calibration factor to within 5% at 410 nm, we have some doubt about the 945 nm calibration because the signals for Jupiter itself were about half of predicted levels. Until we can establish a reliable inflight calibration for 678 and 945 nm, the estimated color temperature should be considered preliminary and subject to significant uncertainty.

9. C. W. Herd *et al, Bull. Amer. Astron. Sot.,* in press.

10. W. D. Smythe *et al, Bull. Amer. Astron. Sot.,* in press.

11. For example, J. Borovicka, in *Meteoroids and their Parent Bodies,* (Astron. Inst. Slovak Acad. of Sci., Bratislava, 1993), derives an excitation temperature of 4000 K for a large terrestrial fireball. Analysis of meteoric production of heat and light was summarized by E. Öpik in *Physics of Meteor Flight* in *the Atmosphere,* (Interscience, New York, 1958).

12, For example, P. M. Millman, in *Solid Particles in the Solar System,* I. Halliday and B. McIntosh, Eds., (Reidel, Dordrecht, 1980), p. 121-128. Whereas terrestrial atmospheric emissions by N and O are weak in the visible region, and contribute little to

meteor spectra, the Paschen and Balmer lines of H should appear in Jovian meteor spectra. Comets scatter sunlight in bands due to molecular radicals; near the PPR filter locations, J.R. Johnson, U. Fink, and S.M. Larson, *Icarus* 60, 351 (1984) show a NH2 feature in the region near 678 and a CN feature near 94S nm. Within 0.2 AU of the sun, atomic lines appear [G.W. Preston. *Astrophys. J. 147, 718 (1967)].* Post-impact spectroscopic observations of Jupiter (P. Drossart *et al, Bull. Amer. Astron. Sot.,* in press) show a Li transition near 678 nm within a few minutes after each impact that could also be present in the initial flash.

13. This suggests that the meteor flashes would have been best detected in the blue, and that if the PPR flashes contain meteor light, we poorly sample the true luminosity of that phase.

14. D. P. Hamilton *et al, Bull. Amer. Astron. Sot.,* in press.

15. P. Drossart *et al, Bull. Amer. Astron. Sot.,* in press.

16.1. de Pater et *al, Bull. Amer. Astron. Sot.,* in press.

17. P. D. Nicholson *et al, Bull. Amer. Astron. Sot.,* in press.

18. V. Meadows, D. Crisp, G. Orton, T. Brooke, and J. Spencer, *Bull. Amer. Astron. Sot.,* in press.

19. H. B. Hammel, *et al, Science,* in press.

20. J. C. Arvesen, R. N. Griffin, Jr., and B. D. Pearson, Jr. *Appl. Optics 8, 2215* (1969).

21. H. A. Weaver et *al, Science,* in press.

22. The research described in this paper was carried out by the Jet Propulsion Laboratory, California Institute of Technology, under a contract with the National Aeronautics and Space Administration. We acknowledge strong support from the Galileo Project in the planning and execution of the Shoemaker-Levy 9 observing sequence, The impact timing predictions of P. Chodas and D. Yeomans (JPL) were essential to the timing of the data acquisition.

Figure legends

Figure 1. Size of Jupiter and impact site location within the Galileo PPR field of view.

Figure 2. Fragment H and L impacts.
Raw signal traces for the two orthogonal polarization channels of the PPR. Differences *in* ambient level of the two channels are due to electronic drift of the zero radiance level; the dark current restoration procedure normally performed was omitted here in order to avoid filter wheel stepping and consequent loss of time resolution. Offsets have been applied to Channel 2 data to facilitate comparison. Sample interval is 0.23 sec.

Figure 3. Fragment Q1 impact.
Raw signal traces for the two orthogonal polarization channels of the PPR for both the 678 and 945 nm filters, which were viewed alternately. Differences in ambient level of the two polarization channels are due to electronic drift; offsets have been applied to facilitate comparison. Sample interval is 1.26 sec for a given filter.

Figure 4. Fragment G impact.
Peak signal levels obtained during the repetitive scanning motion across Jupiter, with a period of 5.3 sec. The average of the two orthogonal polarization channels of the PPR is shown.

Figure 5. Fluxes at 945 and 678 nm for impact Q1.
The two polarization channels were averaged together for each wavelength, and periodic noise in one 678 nm channel removed (see Fig. 3). The relative amplitude of these signals indicates a high temperature for the flash.

Figure 6. Fluxes at 945 nm for the impacts Ci, H, L, and Q1.
Data for G are shown as + symbols.

TABLE 1. Galileo PPR Observations

Fragment	Impact time*	Time observed	λ, nm	Signal Maximum Watt cm^{-2} nm^{-1}	Note
B	See note	199 07:32:00-07:40:00†	945	---	Signal too weak to be seen.
G	199 07:33:32	199 07:32:00-07:40:00†	945	2.1 E-15	Sampled once per 5.3 sec period.
H	199 19:31:58	199 19:11:24-19:52:12	945	1.8 E-15	
L	200 22:16:48	200 22:09:00-22:26:24	945	2.6 E-15	
P	See note		945	---	Recorded but not played back. Signal likely too weak.
Q1	201 20:13:52	201 20:03:36-20:30:36	945	1.1 E-15	Two wavelengths alternate.
			678	3.0 E-15	
R	See note	To be determined	678	---	To be returned early 1995.
S	See note	202 15:21:00-15:59:25	945	---	Event shifted out of observed period.

*Converted to equivalent time for Earthbased observers in UTC: Day of year HH:MM:SS
†Time span covered by data returned to Earth to date.

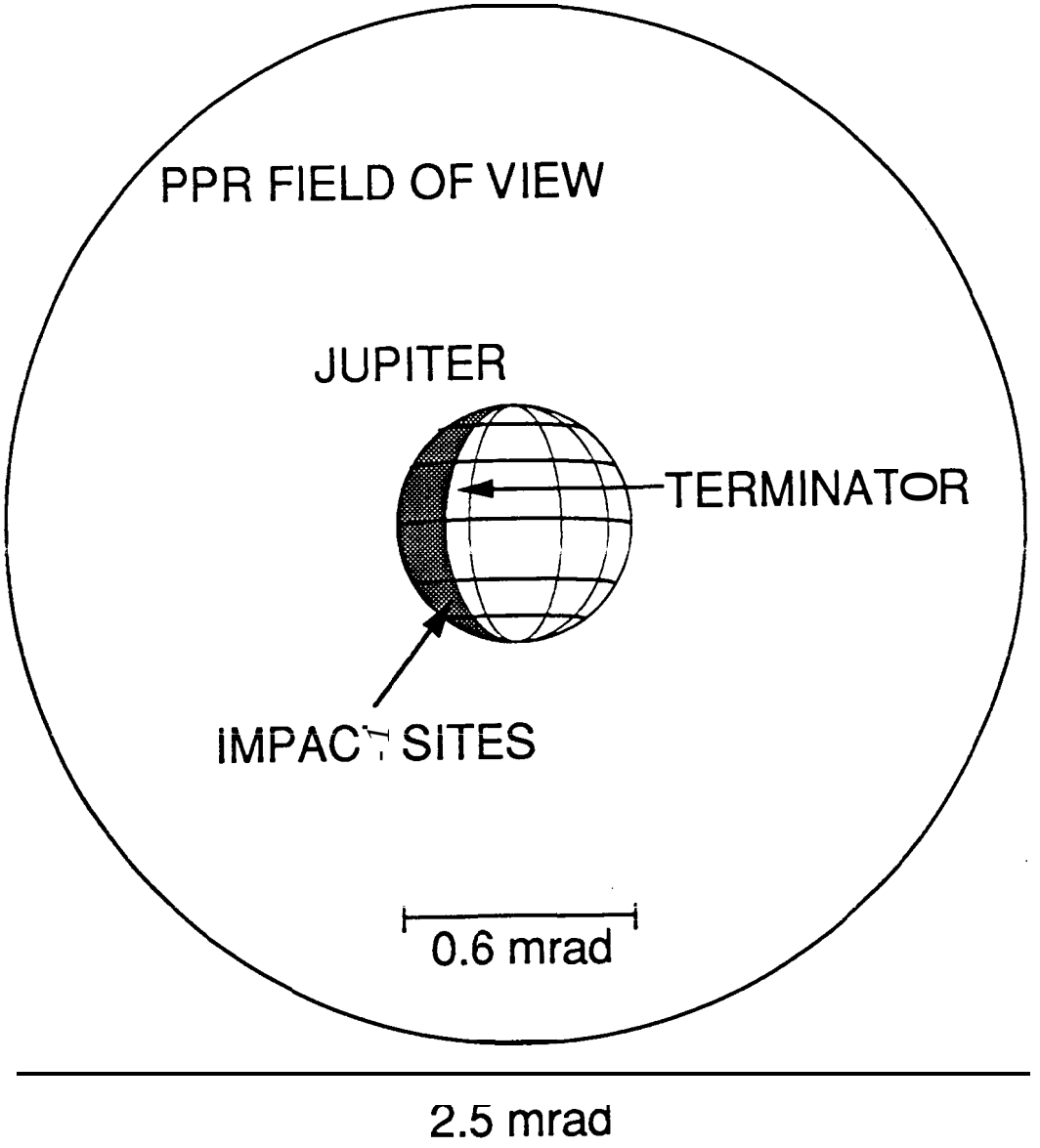
PPR FIELD OF VIEW
JUPITER
TERMINATOR
IMPACT SITES
0.6 mrad
2.5 mrad

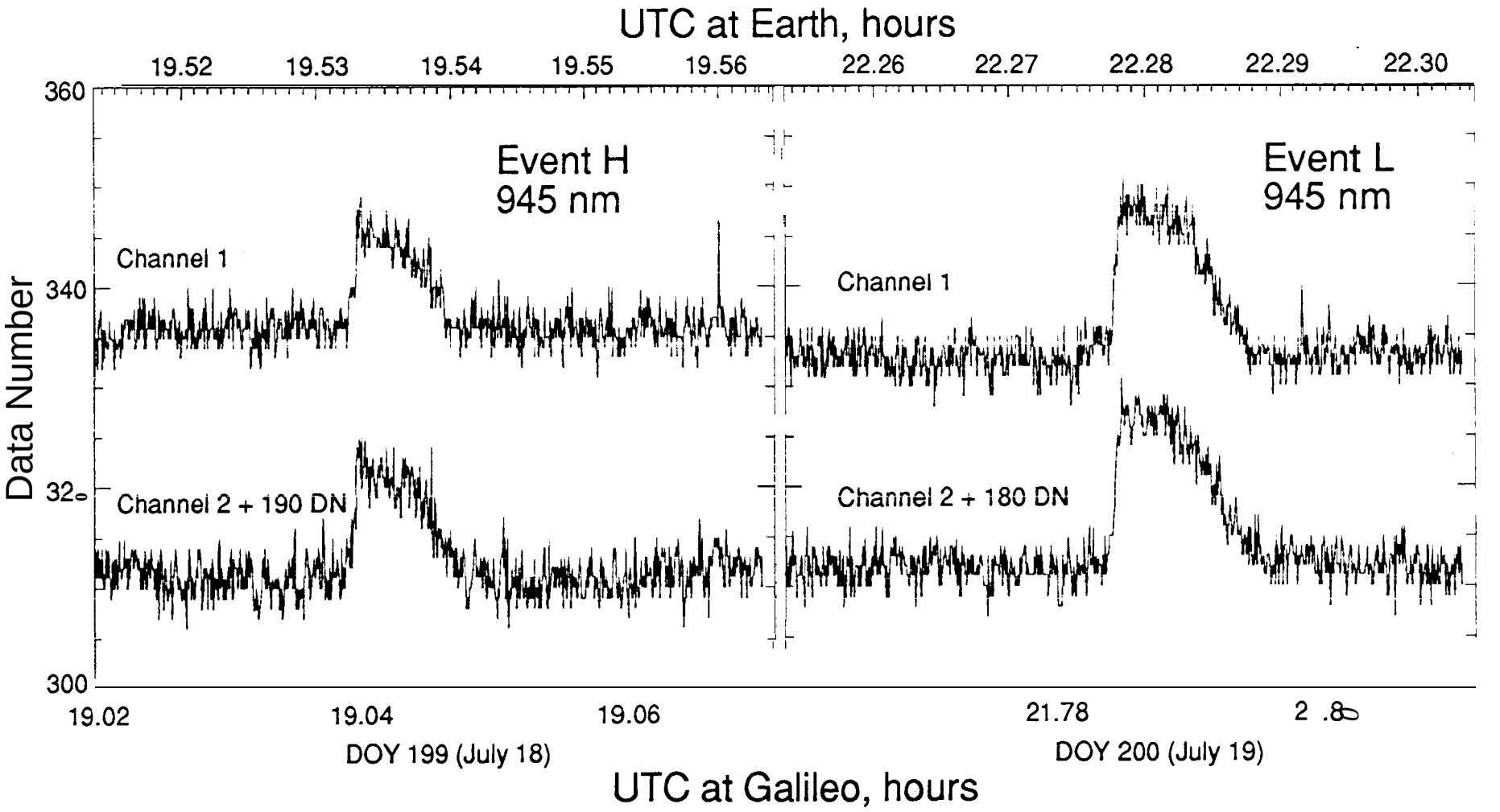
UTC at Earth, hours
19.52
19.53
19.54
19.55
19.56
22.26
22.27
22.28
22.29
22.30
360
340
320
300
Data Number
Event H
945 nm
Channel 1
Channel 2 + 190 DN
Event L
945 nm
Channel 1
Channel 2 + 180 DN
19.02
19.04
19.06
21.78
2 .8
DOY 199 (July 18)
DOY 200 (July 19)
UTC at Galileo, hours

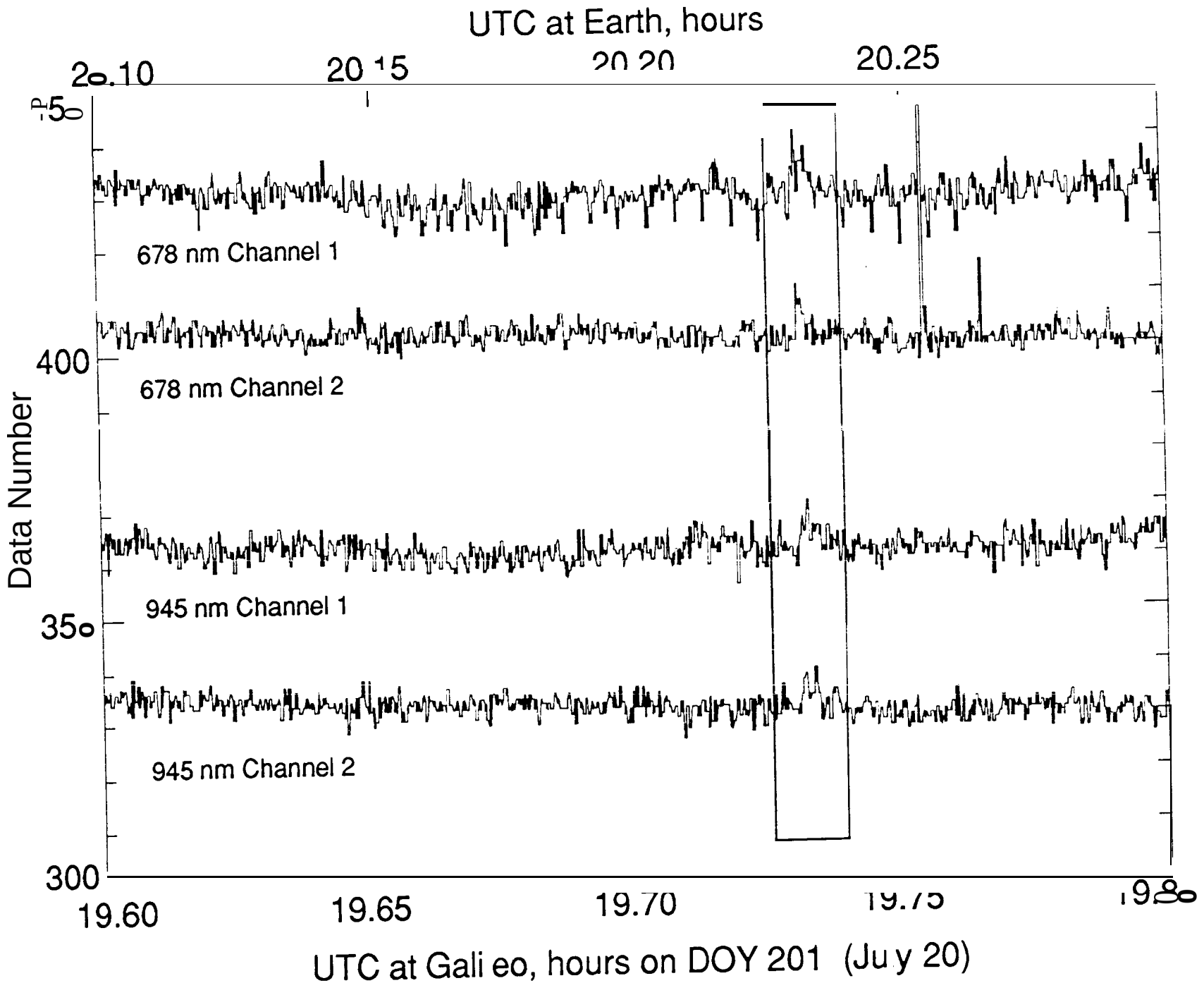
UTC at Earth, hours
20.10
20.15
20.20
20.25
678 nm Channel 1
678 nm Channel 2
945 nm Channel 1
945 nm Channel 2
Data Number
400
350
300
19.60
19.65
19.70
19.80
UTC at Galileo, hours on DOY 201 (July 20)

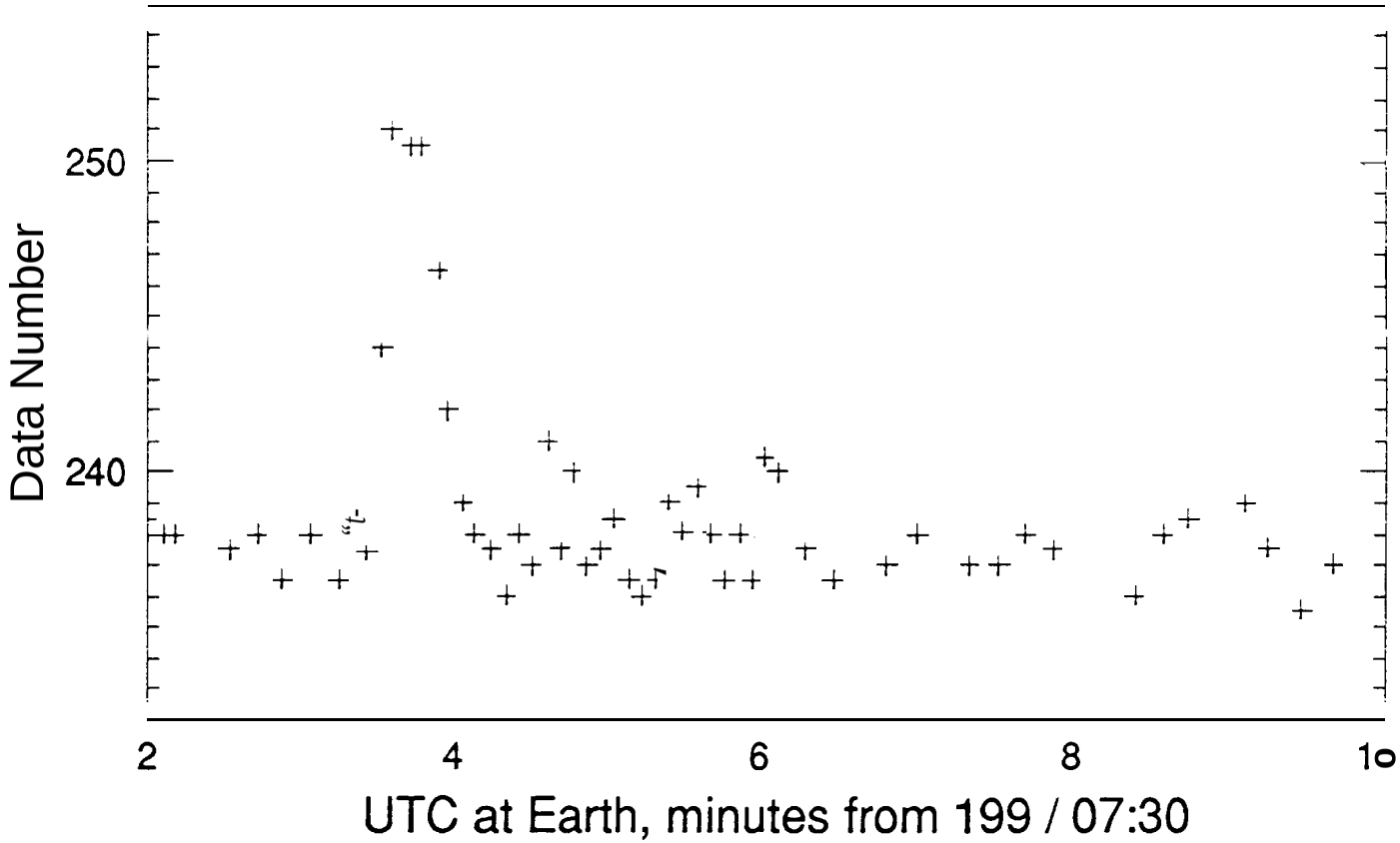
Data Number
250
240
2
4
6
8
10
UTC at Earth, minutes from 199 / 07:30

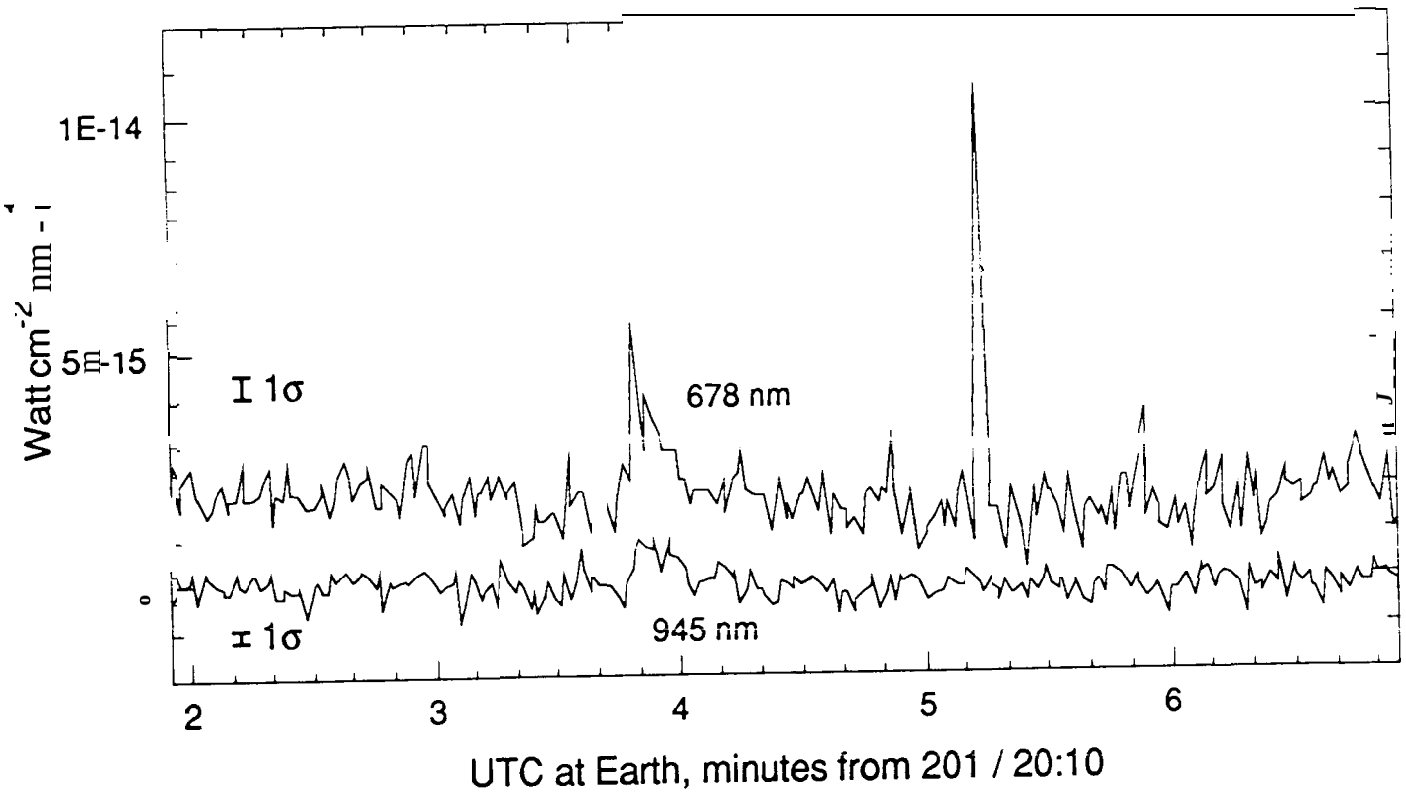
1E-14
5E-15
0
Watt cm-2 nm - 1
I 1σ
678 nm
x 1σ
945 nm
2
3
4
5
6
UTC at Earth, minutes from 201 / 20:10

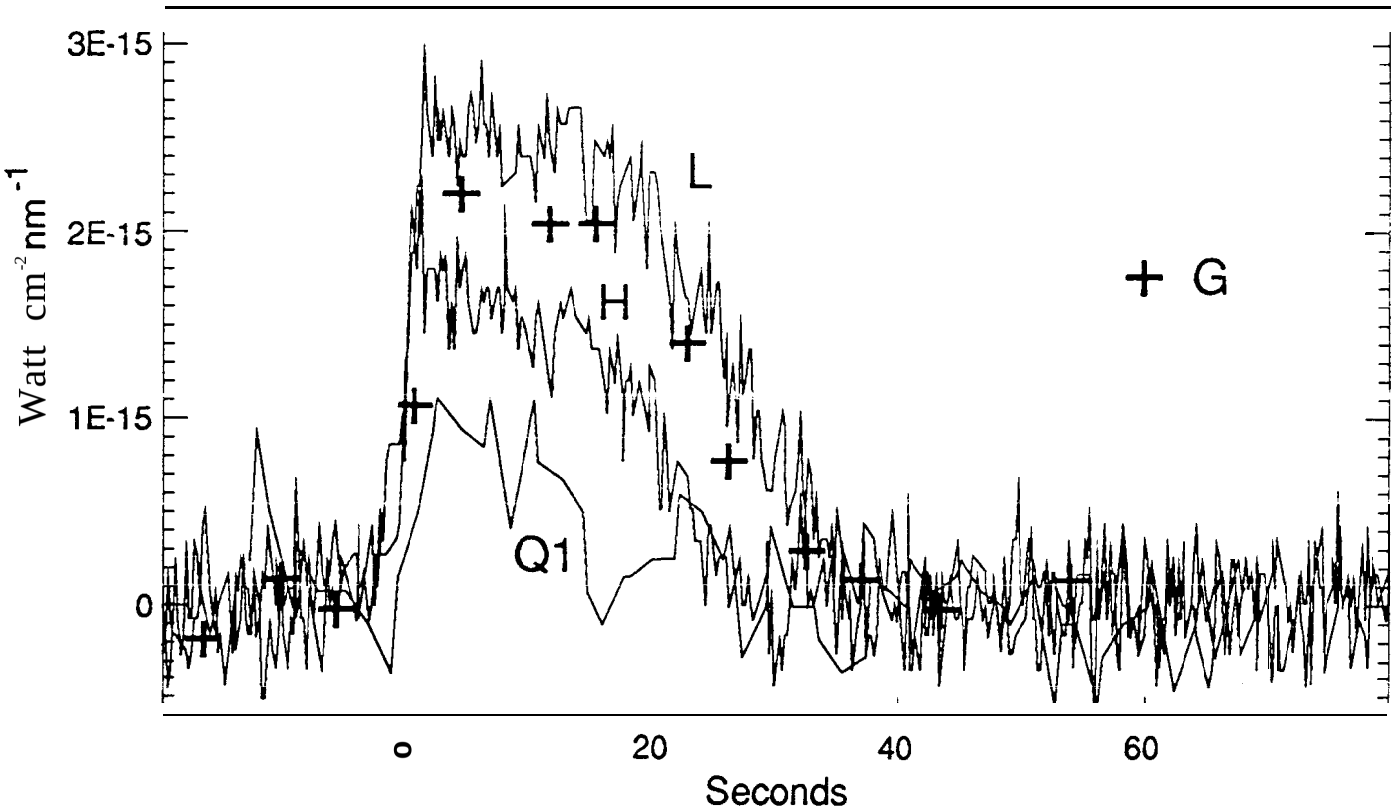
3E-15
2E-15
1E-15
0
Watt cm-2 nm-1
L
H
Q1
+ G
0
20
40
60
Seconds